Deviations in the Thermal Properties of Ultrathin Polymer Network Films

Joseph L. Lenhart* and Wen-li Wu

National Institute of Standards and Technology, 100 Bureau Drive Stop 8541, Gaithersburg, Maryland 20899-8541

Received November 1, 2001

ABSTRACT: Cross-linked epoxy network films were cast onto silicon wafers with a variety of surface treatments. X-ray reflectivity was used to characterize their electron density and thermal expansion in the rubbery state. A transition from "bulk" to "confined" expansion occurs in the range of 200−400 Å, where thinner films exhibit smaller rubbery expansion coefficients. The thermal expansion behavior of the epoxy films was *independent* of the substrate surface treatment, which varied in both surface energy and the strength of bonding interactions with the polymer. The thickest epoxy films displayed typical rubbery thermal expansion values for temperatures above the bulk polymer glass transition temperature. The thinnest epoxy films (<120 Å) exhibited typical glassy expansion values even at temperatures 20−40 °C above the bulk polymer glass transition temperature, *independent* of the surface treatment.

Introduction

The interfacial properties of polymers are known to be different than the properties of bulk polymers. Simulations show that the polymer films confined between two parallel plates exhibit deviations from the bulk conformation when the plate separation is less than twice the polymer radius of gyration (R_g).[1] Other simulations have shown that density fluctuations can extend over several monomer units, while the polymer coils are slightly flattened in the vicinity of the surface and approach the bulk Gaussian configuration[2] after $(2-3)R_g$. Using reflectivity, Wallace et al. were not able to detect deviations in thin film polymer mass density relative to the bulk.[3] However, this measurement was a course measurement of polymer density having roughly 1% accuracy. Density fluctuations smaller than 1% could dramatically change the properties of thin polymer films. More recently, X-ray reflectivity has been used to detect molecular layering in a liquid film on a solid substrate[4] and subtle density fluctuations in thin poly(methyl methacrylate) (PMMA) films adhered to silicon wafers.[5] In addition to changes in polymer conformation and density, interfacial mobility can be different than mobility in the bulk. Preferential segregation of low molecular mass polymer fractions, chain ends to the interface,[6] and lower entanglement density[7] could reduce the glass transition temperature in the interfacial region. Tanaka et al. observed enhanced mobility at the air/polystyrene interface due to segregation of end groups,[8] but only for molecular masses (M_n) below 40 000. Calvert suggests that end group segregation at the polymer/substrate interface might induce stretched polymer conformations, leading to slower dynamics and diffusion processes.[9]

Polymer thin films have been used extensively as model systems to probe interfacial effects on the polymer mobility. Both dewetting,[10,11] and temperature-dependent thickness measurements[12] illustrated that thin polystyrene films can exhibit polymer mobility even at temperatures well below the bulk polymer glass transition (T_g). Subsequent work by a wide range of groups has shown that the thermal properties in thin polymer films can be different than the bulk and will dramatically depend on the polymer/substrate interactions.[13−27] For PMMA the thin film T_g can increase on hydrophilic surfaces[13,14] and decrease on hydrophobic surfaces.[14,15] The T_g of polystyrene films has been observed to decrease with decreasing film thickness[13,16−20] over a wide range of substrates. Wallace et al. observed an increase in the T_g for polystyrene films on hydrogen passivated wafer surfaces.[21] In contrast to the results of Wallace et al.,[21] Keddie et al. observed that the T_g of thin polystyrene films on hydrogen passivated silicon surfaces was lower than the bulk T_g.[22] However, the experiments by Keddie et al.[22] were conducted in atmosphere. Wallace et al.[21] suggested that the passivated wafer surface is unstable in atmosphere and can rapidly oxidize. It is therefore possible that Keddie et al.[22] had a polystyrene film supported on an oxide layer where the film T_g has been shown to decrease with decreasing thickness.[12,17,20] The experiments of Wallace et al. were conducted under vacuum, where the passivated wafer surface is less likely to oxidize.[21] Using the same substrate surface treatment as Keddie et al.,[22] Kawana and Jones[16] showed that the rubbery coefficient of thermal expansion (CTE) for polystyrene films is independent of the film thickness. The glassy CTE increases with decreasing film thickness,[16] leading to a decrease in the fragility of the transition.[16] However, Wallace et al. showed that for polystyrene films the glassy CTE remains constant while the rubbery CTE decreases with film thickness.[21] While the exact differences in substrate surface chemistry are unclear in these references,[16,21,22] these articles illustrate how changes in the substrate surface treatment can have a dramatic impact on the observed glass transition temperature, glassy CTE, and rubbery CTE for thin polymer films. Further illustrating the importance of substrate surface character, Fukao and Miyamoto observed a decrease in the thin film glass transition temperature for polystyrene on aluminum surfaces yet claim that the glassy expansion increases while the rubbery expansion decreases, with decreasing film thickness.[19] Using a

* To whom correspondence should be sent: e-mail jlenhart@nist.gov; phone 301-975-4769.

10.1021/ma011903v
Published on Web 05/15/2002

silicon wafer coated with a monolayer of silane coupling agents, Fryer et al. showed that T_g of polystyrene and PMMA films can either increase or decrease with decreasing film thickness, depending on the substrate surface energy.[23] In most cases, changes in the apparent thin film T_g have been roughly 20 °C or less relative to the bulk value. However, van Zanten et al. showed that for poly(2-vinylpyridine) the apparent T_g of thin polymer films can increase by as much as 50 °C above the bulk value,[24] due to strongly favorable polymer/substrate interactions. More recently, the glass transition of poly(hydroxystyrene) (PHS) films was shown to increase by more than 50 °C in films strongly grafted to the substrate.[20] The rubbery CTE of PHS films also exhibited a dramatic dependence on the substrate surface characteristics[25] even for films as thick as 1000 Å.

The type of confining interfaces in the polymer film will also influence the thermal properties. Forrest et al. observed the T_g of free-standing polystyrene films to decrease by as much as 70 °C in the thinnest films,[26] suggesting that a mobile layer of polymer at the air interface is the cause of the T_g suppression. For polystyrene supported on SiO_x surfaces the decrease in T_g is smaller.[17,20] For polystyrene films supported at both interfaces with an immobile polyimide layer, a T_g change in the films could not be detected.[27] However, the rubbery coefficient of thermal expansion (CTE) decreased significantly with decreasing film thickness.[27]

It is clear that the thermal properties of polymer films are dependent on the polymer/substrate interactions. These changes in the apparent thin film glass transition and CTE's are observed to propagate a few R_g from the surface in most cases. However, surprisingly long-range effects have been observed for diffusion processes. Zheng et al. measured diffusion of d-polystyrene in h-polystyrene matrices and found that the diffusion coefficient near a silicon wafer substrate was dramatically reduced. This was attributed to a larger monomeric friction coefficient in the interfacial region.[28] Similar decreases in polymer/polymer diffusion coefficients were observed to propagate $(5-10)R_g$[29,30] and even $20R_g$ from the substrate surface.[31]

Most of the work to date probing the thermal properties of ultrathin polymer films has focused on monodisperse thermoplastic polymers (predominantly polystyrene-based polymers and poly(methyl methacrylate)). Because of the limited number of polymers studied, it is important to broaden the thin film research in order to determine whether the trends observed for polystyrene and PMMA are general to a wide range of polymer systems. One class of polymer films that has not been adequately studied is cross-linked polymers. Interfacial properties of cross-linked polymers are important in technical applications such as fiber-reinforced composites, nanocomposites, artificial tissue scaffolds, electronics packaging, antireflective coatings, and general adhesive applications. One current approach for understanding the polymer network properties near an interface has focused on determining the chemical composition profile of the resin monomers near the surface. Palmese and McCullough have shown that the concentration profiles can vary in the interfacial region due to preferential segregation of one of the network components to the substrate.[32,33] Once the interfacial stoichiometry is known, the interphase properties can be estimated through a calibration with the bulk resin properties as a function of composition.[34] Yim et al. investigated epoxy films with neutron reflectivity.[35] Hydrogenated epoxy films were swollen with a deuterated solvent, and the cross-link density of the film was extracted from the deuterium profile in the layer.[35] They found a large increase in swelling near the air/epoxy interface but no significant change near the substrate. This was interpreted as being due to preferential segregation of hardener to the air interface. VanLandingham et al. used atomic force microscopy nanoindentation to probe variations in the network modulus near the substrate;[36] however, the technique was limited in that the indentations could not be made close to the substrate surface. While the monomer composition profile is critical to the network interfacial properties, relating chemical composition to the physical properties of the interfacial region is difficult without also understanding how monomer orientation, polymer/substrate bonding, and confinement influence the network structure and properties in this region.

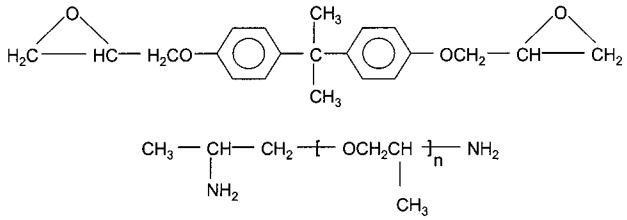

Figure 1. Structure of the resin monomers. The top is DGEBA, and the bottom is D400.

In this work we use X-ray reflectivity to probe the thermal properties of thin cross-linked polymer films adhered to silicon wafers. The silicon wafer surface treatment was varied to adjust both the surface energy and the strength of the polymer/substrate bonding. We show that the rubbery coefficient of thermal expansion decreases with the film thickness, *independent* of the wafer surface treatment. In addition, "glassy" expansion behavior was observed in films thinner than 120 Å, even at temperatures 20−40 °C above the bulk polymer T_g, *independent* of the wafer surface treatment. This illustrates that cross-linked polymer films can behave very differently than linear chain polymer films, where the thermal properties are strongly dependent on the substrate characteristics. We propose that the network cross-links effectively screen the influence of the polymer/substrate interactions. The network was composed of an epoxy monomer cross-linked by a diamine hardener (see Figure 1).

Experimental Section

Unless otherwise stated, all chemicals were used as obtained from Aldrich Chemical Co. (Milwaukee, WI).[37] Silane coupling agents were used as received from Gelest (Tulleytown, PA).

The cross-linked polymer network used in this study was an amine-hardened epoxy system composed of a stoichiometric ratio of diglycidyl ether of bisphenol A (DGEBA, Tactix 123, Dow Chemical Co.) mixed with poly(propylene glycol) bis(2-aminopropyl ether) (Jeffamine D400, Aldrich Chemical Co.). The molecular mass of the hardener was 400 g/mol. The resin monomers are shown in Figure 1. The two components were mixed thoroughly with a mechanical stirrer prior to use. The epoxy films were spun-cast onto a silicon wafer from propylene glycol methyl ether acetate (PGMEA). Before dissolving the monomers in PGMEA, the resin was partially cured at 90 °C for 30 min in order to build up the polymer viscosity. This was necessary, as the uncured epoxy will immediately dewet the substrate. Once cast onto the silicon wafer the films were cured at 20 °C for 12 h under vacuum. This was followed by curing

under vacuum at (40, 60, 80, and 100) °C for 3 h at each temperature. Finally, the resin was postcured at 150 °C for 3 h under a vacuum of $10^{-4}-10^{-5}$ Pa. The vacuum was required to completely remove residual PGMEA, which has a boiling point near 140 °C. The slow cure cycle was used to allow ample time for the relaxation and cure of the spun-cast network. The T_g of the bulk resin ranged from 35 to 45 °C, as measured by differential scanning calorimetry (DSC). The postcure temperature was chosen to be above the highest measurement temperature. The cured films were smooth with roughness less than 10 Å in all cases as determined by X-ray reflectivity.

The surface of the silicon wafer was modified by three different treatments. These treatments were chose to adjust both the surface energy and the bonding interactions between the polymer and substrate. For the first treatment, the wafer was exposed to ultraviolet (UV) ozone for 2 min, followed by etching in hydrofluoric acid buffer to strip the oxide layer. The oxide layer was redeposited on the wafer by an additional UV ozone exposure for 2 min. This treatment leaves a high-energy silicon oxide layer (SiO_x) on the wafer surface with a water contact angle less than 5°. The SiO_x layer contains hydroxyl groups, which have the potential to hydrogen bond with the cured epoxy network.

For the second surface treatment, a thin layer of (aminopropyl)triethoxysilane coupling agent (APS) was deposited onto the silicon wafer surface. The APS-coated surface had a water contact angle ranging from 45° to 55°. The amine group on APS can participate in the cross-linking reaction with the epoxy (DGEBA) monomer during resin cure.

In the third surface treatment, the wafer was coated with a thin layer of propyltriethoxysilane coupling agent (PTS). The PTS-coated surface has a water contact angle ranging from 80° to 110°. The PTS layer can interact with the polymer through van der Waals type interactions.

Before depositing the silane coupling agent layers on the silicon wafer, the wafers were cleaned for 2 min with UV ozone exposure. The oxide layer was stripped in hydrofluoric acid and then redeposited by further UV ozone exposure (similar to the SiO_x treatment described above). The clean wafers were then dipped in coupling agent solutions. Fifteen minutes was allowed for adsorption of the coupling agents onto the wafer surface. After dipping, the wafer was heated at 100 °C for 30 min. To remove the physically adsorbed coupling agent material, the coated wafers were immersed in boiling water for 5 min, followed by a rinse with spectral grade acetone. The coupling agent layers were not continuous but consisted of closely packed islands of coupling agent material with RMS roughness ranging from 10 to 15 Å as measured by atomic force microscopy. X-ray reflectivity on the silane coated wafers also showed roughness of 10−15 Å.

The silane coupling agent solutions consisted of 250 μL of the silane coupling agent dissolved in 50 mL of an ethanol/water mixture with an ethanol volume fraction of 95%. A 125 μL aliquot of 1 mol/L hydrochloric acid was added to the ethanol/water mixture. The solution was stirred at room temperature for 1 h to allow the coupling agents to hydrolyze. The silicon wafers were then dipped into this solution.

Thermal expansion measurements were conducted on an X-ray reflectometer (Scintag) with 1.54 Å radiation from a Cu Kα source. The samples were held at 140 °C under a vacuum of 10^{-6} Pa for 6 h prior to any measurements. Then the thickness was measured starting at 140 °C cooling to 20 °C and then heating back to 140 °C. For all the films the cooling and heating cycles overlapped, indicating a stable polymer film. Before each thickness measurement the sample was annealed at the measurement temperature for 1 h.

Results and Discussion

Figure 2 shows typical reflectivity data for an epoxy film at several different temperatures. The dramatic drop in reflectivity near $q = 0.03$ Å^{-1} is due to the silicon critical edge, where the X-ray radiation begins to penetrate the silicon wafer as the angle of incidence

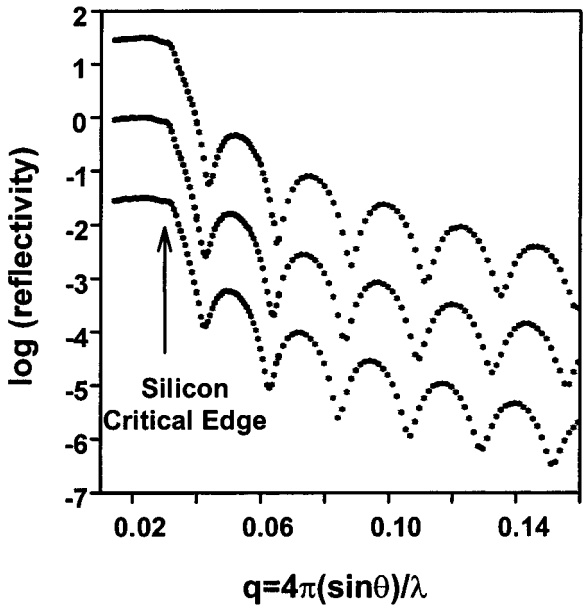

Figure 2. Specular X-ray reflectivity curves for a typical DGEBA/D400 film on a SiO_x-coated silicon wafer. The top curve is from the film at 20 °C (260 Å), the middle curve is from the film at 70 °C (266 Å), and the bottom curve is from the film at 150 °C (273 Å). The curves are offset for clarity. The standard uncertainty in the data points is less than the symbol size.

increases. Figure 2 illustrates the angstrom level sensitivity of reflectivity to film thickness. The film thickness is measured by $2\pi/\Delta q$ where Δq is the periodicity in q. When the temperature increases, the film thickness increases due to thermal expansion, and Δq of the reflected intensity decreases. The last fringe in Figure 2 clearly illustrates the decrease in Δq, as the film thickness increases. For all the thickness measurements, the reflectivity was measured to q values of 0.35 Å^{-1}. However, the high q data are not displayed in Figure 2 for clarity. The best fit to the reflectivity data was obtained by using a model with a single epoxy layer of uniform density and a silicon oxide layer 15−25 Å thick on the wafer surface. We acknowledge that subtle density changes could occur in the epoxy films as were observed by X-ray reflectivity in PMMA thin films.[5] However, detecting these density variations requires measuring the reflectivity at significantly higher q values. Because of time constraints (each thickness measurement at a particular temperature takes 3 h), we limited the q range in our measurements to 0.35 Å^{-1}.

Figure 3a−f shows typical thickness vs temperature plots for both a thick and thin epoxy film on the SiO_x (Figure 3a,b), PTS (Figure 3c,d), and APS (Figure 3e,f) coated wafer surfaces. The thickest epoxy films (Figure 3a,c,e) exhibit a linear thickness change with temperature above the bulk polymer glass transition temperature (from 40 to 140 °C). For these thick films, the coefficient of thermal expansion (CTE) over this temperature range was $(4.1 \pm 0.3) \times 10^{-4}$ K^{-1}, a value typical for rubbery polymer thin film CTE when corrected with Poisson's ratio. The bulk value for the glass transition of this epoxy system is ≈40 °C. Since we only measured a few thickness values in the glassy region, the thick film glass transition temperature cannot be adequately determined by a break in the thickness vs temperature plots.

In contrast to the thickest epoxy films (which expand with typical rubbery CTE values at temperatures

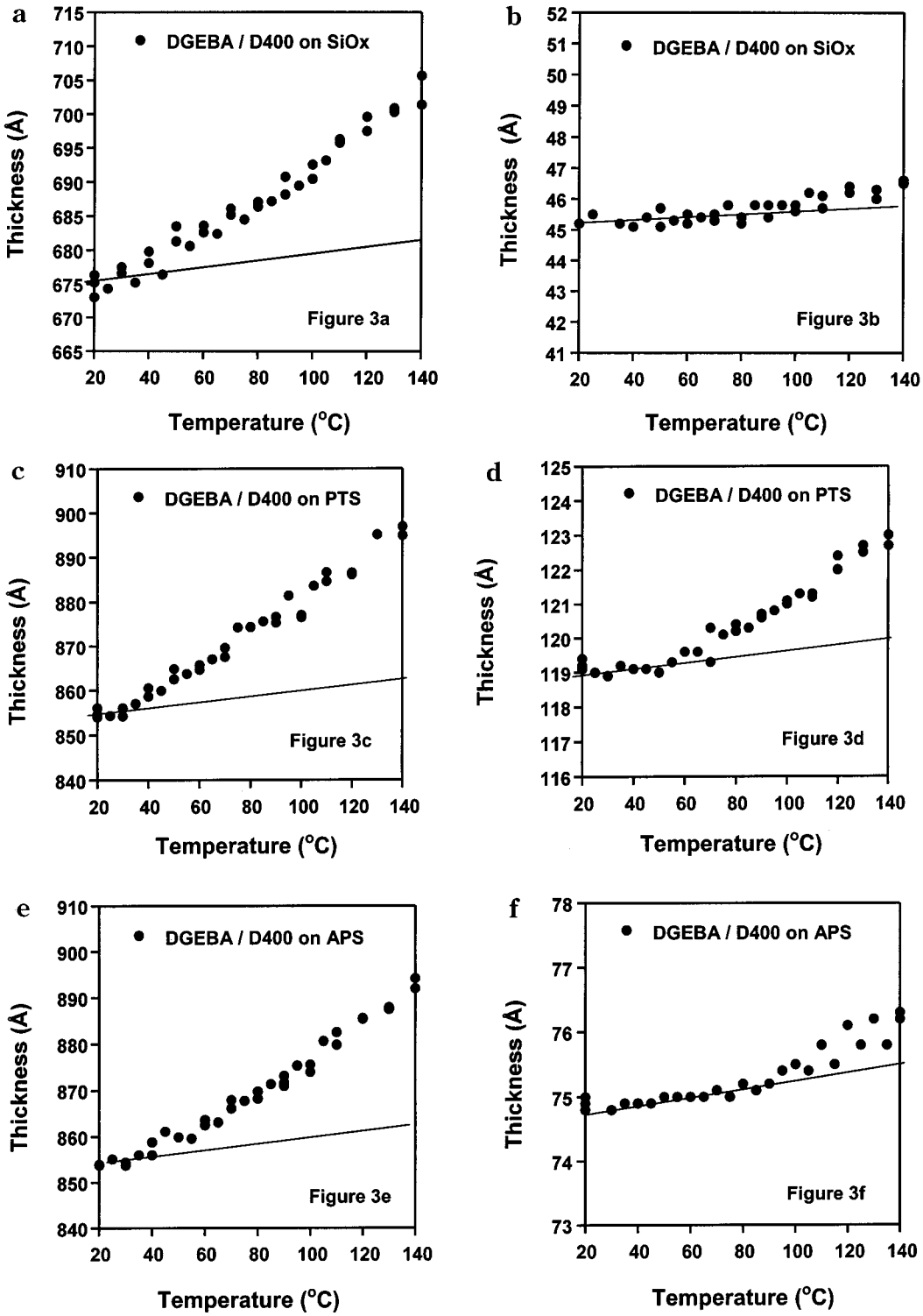

Figure 3. Epoxy film thickness plotted as a function of temperature: (a) a thick film on a SiO_x–coated surface, (b) a thin film on a SiO_x-coated surface, (c) a thick film on a PTS-coated surface, (d) a thin film on a PTS-coated surface, (e) a thick film on an APS-coated surface, (f) a thin film on an APS-coated surface. The line represents the expansion of a typical glassy polymer film with a CTE value of 0.8×10^{-4} K^{-1}. The thin polymer films exhibit glasslike expansion even at temperatures 20−40 °C above the bulk polymer glass transition. The cooling and heating cycles overlap, and both are shown in the data points. The data scatter represents the relative uncertainty in the thickness.

greater than the bulk polymer T_g of 40 °C), the thin epoxy films (Figure 3b,d,f) did not show "rubbery" thickness changes until temperatures >60 °C. To guide the eye, lines are added in Figure 3a−f with a CTE value of 0.8×10^{-4} K^{-1}, a typical expansion value for glassy polymer films.[16,21,24,27] The lines clearly show that the thin epoxy films (Figure 3b,d,f) exhibit "glasslike" expansion behavior on each type of wafer surface, even for temperatures >60 °C (roughly 20 °C above the bulk polymer T_g). Unlike the thick films, the thinnest films (Figure 3b,d,f) showed a distinct break in the thickness vs temperature plots, indicative of an apparent glass transition temperature for these films. This break occurs at temperatures ranging from 20 to 40 °C above the DSC

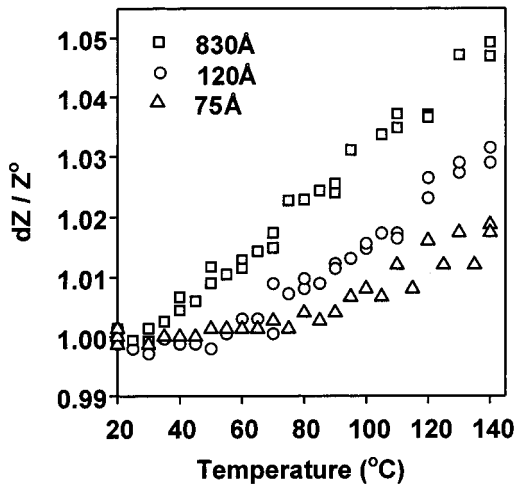

Figure 4. Fractional thickness change as a function of the film temperature for typical epoxy films. The rubbery CTE decreases with the epoxy film thickness. Both cooling and heating cycles are shown in the plot. The standard uncertainty associated with the normalized thickness data is less than ±0.005 in all cases as is evident by the data scatter.

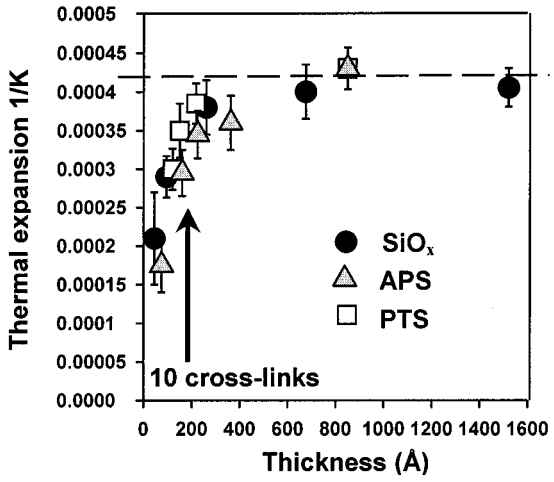

Figure 5. Thermal expansion (for temperatures between 40 and 140 °C) plotted as a function of the film thickness. The filled circles show the CTE for epoxy films on a SiO_x-coated wafer surface. The triangles show the CTE for epoxy films on an APS-coated wafer surface. The squares show the CTE for epoxy films on a PTS-coated wafer surface. Error bars reflecting the uncertainty in the thermal expansion were estimated from the scatter in the thickness vs temperature plots for each film.

value for the bulk polymer T_g. However, an increase in the apparent T_g values for these thinnest films can only be inferred from these data, because a distinct break was not observed in the thicker films, presumably due to the lack of data points below the bulk epoxy T_g. A decrease in the fragility of the glass transition is not a feasible explanation for the lack of a break in the thickness vs temperature plots for the thickest films, since a decrease in the transition fragility is expected in thinner films not thicker films.[16] A broadening of the transition could contribute to the small thickness changes between 20 and 60 °C in the thinnest epoxy films. For example, Kawana and Jones observed that the glass transition for thin polystyrene films broadened toward lower temperatures, and the fragility of the T_g decreased due to an increase in the glassy CTE values with decreasing film thickness.[16] A broadening of the α relaxation process has also been observed for thin PMMA films relative to thicker films.[38]

While an accurate measure of the epoxy film glass transition is difficult, the relative thickness changes of the films can be directly compared. Figure 4 shows the thickness change (normalized with the film thickness at 20 °C) as a function of temperature for three different epoxy films. The top curve is for an 830 Å epoxy film on PTS-coated surface. The middle set of data is for a thinner epoxy film (120 Å) on PTS. The bottom data set shows a 75 Å epoxy film on APS. The thin epoxy films clearly exhibit smaller fractional expansion, illustrating that the rubbery CTE of the thin epoxy films is reduced.

Figure 5 plots the total thermal expansion over the temperature range from 40 to 140 °C vs the thickness of the epoxy film at 20 °C. Thicker films exhibited similar expansion behavior with CTE values of $(4.1 \pm 0.3) \times 10^{-4}$ K^{-1}, which is consistent with a bulk rubbery thermal expansion when corrected with Poisson's ratio. A transition occurs from "bulklike" to "confined" expansion between 200 and 400 Å, with thinner films displaying smaller expansion. Neutron scattering studies on a similar epoxy resin provide a length scale of ≈20 Å for the end-to-end distance between cross-links.[39,40] Figure 5 illustrates that the transition from "confined" expansion to "bulk" expansion corresponds to a range of 10−20 cross-link junctions.

Figure 5 illustrates that the thermal expansion of the epoxy films was *independent* of the wafer surface treatment. The epoxy films exhibited the same decrease in the rubbery CTE with decreasing film thickness whether the wafer surface was coated with SiO_x, APS, or PTS. As mentioned in the Experimental Section, the SiO_x surface had a water contact angle <5°, and the surface hydroxyl groups can interact with the epoxy network through hydrogen bonding. The APS surface had water contact angles between 45° and 55°, and the amine functional end groups on the coupling agent can cross-link with the epoxy monomers during cure. The PTS-coated surface had water contact angles between 80° and 110° and can only interact with the network through van der Waals forces. As mentioned in the Introduction section of this paper, the thin film thermal properties for linear chain polymers dramatically depend on the substrate/polymer interactions. Figure 5 clearly shows that the rubbery CTE for these network films is *independent* of the substrate surface treatment. We propose that for polymer networks the cross-link structure of the film/interface will dominate or dampen the influence of the polymer/substrate interaction. If this is true, then the deviations in the thermal properties of polymer network films/interfaces could have a dependence on the molecular weight between cross-links.

While the thermal expansion values in Figure 5 are obtained by measuring changes in the total film thickness, it is possible that the reduction in the CTE is due to a reduced mobility layer in the thin film. Variations in the polymer film mobility near interfaces have been used to explain deviations in the thin film thermal properties. For example, a liquidlike layer at the polymer/air interface was postulated as the cause of the observed decreases in the glass transition temperature for thin polymer films.[14,16,22] The dramatic decrease in T_g for free-standing polystyrene films confirms that the presence of the polymer/air interface leads to a reduction in the thin film T_g.[26] Molecular dynamics simulations of glassy polymer films illustrated a less dense and more mobile layer at a polymer/vacuum interface.[41] However, positron annihilation lifetime spectroscopy[42] and surface

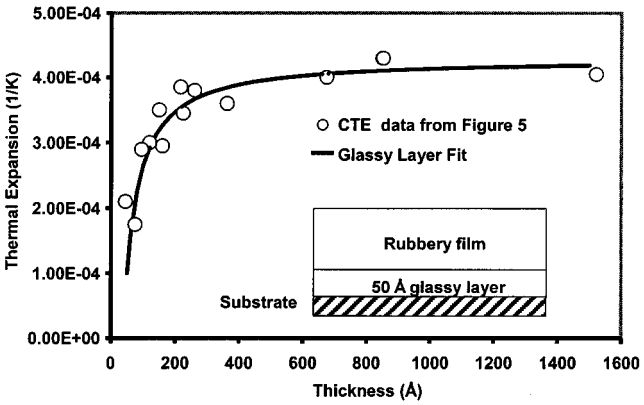

Figure 6. A model assuming a thin "glassy" layer near the substrate surface can predict the thin film rubbery expansion data. The circles represent the CTE data from Figure 5. The line shows the fit to the data using eq 1 and assuming a 50 Å thick "glassy" layer with a CTE of 1.0×10^{-4} K^{-1}. The inset is a schematic of the proposed model.

modulation atomic force microscopy measurements[43] showed that the surface glass transition of the polymer film does not deviate significantly from the bulk value, providing evidence against the existence of a liquidlike layer near the air interface. Near-edge X-ray absorption fine structure (NEXAFS) was used to measure the free surface relaxation of polystyrene and complete relaxation was not seen for temperatures below the bulk polymer T_g, providing further evidence against a liquidlike layer at the air interface.[44] However, recent NEXAFS measurements showed that the surface relaxation of oriented polystyrene was somewhat faster than the bulk relaxation, supporting the idea of a more mobile layer at the air surface.[45] A layer of decreased mobility near the substrate surface has been used to describe the observed increases in the glass transition temperature of thin polymer films.[21,24] Molecular dynamics simulations have shown that the polymer mobility can be either reduced or enhanced near a surface by tuning the polymer/surface interactions.[46] A simple model can be used to fit the data in Figure 5. This model assumes a glassy layer near the substrate surface, while the remainder of the film retains rubbery expansion behavior:

$$\alpha_{film} = \alpha_{gl}\left(\frac{Z_{gl}}{Z}\right) + \alpha_{rl}\left(\frac{Z - Z_{gl}}{Z}\right) \qquad (1)$$

where α_{gl} and α_{rl} are the thermal expansivity for the glassy layer near the substrate and the rubbery layer for the rest of the film, Z_{gl} is the thickness of the glassy layer near the substrate, Z is the total film thickness, and α_{film} is the measured thin film expansion (data from Figure 5). While this is only a simple model, and it is more likely that a gradual change in the thermal properties occurs normal to the substrate, an adequate fit to the data is obtained with a Z_{gl} thickness between 40 and 60 Å, assuming a typical glassy expansion value of 1.0×10^{-4} K^{-1} for α_{gl} and using the plateau value for thick film rubbery expansion from Figure 5 as the $\alpha_{rl} = 4.2 \times 10^{-4}$ K^{-1}. Figure 6 shows the data from Figure 5 and the fit to the data using the glassy layer model, eq 1. The inset in Figure 6 shows a schematic of the proposed model. The thickness of this glassy layer corresponds to $\approx$2−3 end-to-end cross-link junctions.[39,40]

We have no evidence that the cross-link density of the thin epoxy films is different than the cross-link density for the thick films. The electron density measured by the X-ray reflectivity was the same for both thick and thin films within the experimental error. In addition, swelling the layers in deuterated acetone and analyzing the acetone uptake with neutron reflectivity showed that both thick and thin films have the same acetone uptake, which is also uniform across the film thickness except for the top 25 Å layer. An excess of acetone existed in a thin 25 Å layer near the air interface. In all the dry films a uniform electron density through the film thickness provided the best fit to the X-ray reflectivity data. Beck Tan et al. used neutron reflectivity on a model epoxy/D400 resin system with a deuterated epoxy monomer and saw some interfacial epoxy segregation, but only in at most the first monolayer near the silicon wafer.[47] However, this small interfacial region of monomer segregation is difficult to measure by neutron reflectivity without accurately knowing the thickness and neutron scattering length density of the silicon oxide layer on the wafer. With the epoxy films in this study, the polymer viscosity was increased by partially curing the network before spin-casting, making it unlikely that significant monomer segregation occurs. In addition, segregation of monomers to the interfacial region would lead to off-stoichiometric network cure and cause a decrease in the interfacial cross-link density, leading to larger thermal expansion and a decrease in T_g. If segregation was an issue, we would expect the surface treatment to influence this segregation, but there was no such effect. Since the resin monomers are relatively monodisperse, in the absence of significant segregation the interfacial cross-link density will not change.

One possible explanation for the reduced expansion in the thin films is an increase in the polymer density near the substrate. We could not detect any density changes with reflectivity. However, small density changes (<1%) are not detectable without collecting data to significantly higher q values than in this study. A small density change of ∼1% in the thin layer near the substrate could significantly raise the glass transition temperature of that layer[18] and reduce the thin film expansion. Another possible explanation for the confined expansion in thin network films is orientation of the network molecules near the surface. This would allow the hydroxyl groups on reacted epoxy monomers to hydrogen bond more effectively with each other and constrain the mobility. This has been observed in linear chain polymer systems. Frank et al. observed more extensive hydrogen bonding in thin poly(methylhydroxystyrene) films on silicon wafers and suggested that chain orientation near the surface allowed for alignment of hydroxyl groups.[48] Increased hydrogen bonding is known to increase the glass transition temperature of polymer blends.[49,50] Extensive orientation and layering of small molecular mass liquid films, on silicon wafers, has been observed by X-ray reflectivity.[51,52] Fluorocarbon lubricant layers have also been observed to orient near a substrate.[53] It may be possible to probe for orientation in the epoxy films by using sum-frequency generation (SFG) or fluorescence anisotropy measurements with a dye probe dissolved in the epoxy resin. SFG has been used to detect orientation of polystyrene at the air and substrate interfaces.[54,55]

Polymer networks used in electronics packaging and fiber reinforced composites are typically processed using injection molding techniques. Often, the network is

cured significantly during the injection process, leading to processing induced stress, strain, and orientation. The epoxy films used in this study were partially cured before dissolving the polymer in PGMEA and spin-casting to build up the resin viscosity and prevent dewetting. It is important to discuss the potential impact of this partial curing on the structure of the network films. We believe that the predominant impact of the partial curing is to eliminate the potential for significant monomer segregation at the interfaces in the film. As mentioned above, monomer segregation would lead to off-stoichiometric cure, causing a decrease in the film T_g and an increase in the CTE. However, the spinning process can induce deviations in stress, strain, and orientation of polymer films. For example, anomalies in the refractive index of spun-cast polystyrene films have been attributed to segmental orientation induced by the spinning process.[56] These anomalies, however, were annealed away at temperatures above T_g. Spun on films are potentially subjected to a residual shear stress. Pae et al. used an extension of Gibbs−Dimarzio theory and showed that stress will cause a decrease in the T_g of the stressed polymer relative to an unstressed polymer.[57] Strain can also cause the polymer glass transition temperature to increase[58] or decrease.[59] It was proposed that two competing factors contribute to the observed changes in T_g with strain:[60] an increase in free volume due to the strain leads to decreasing T_g, and a decrease in the polymer conformational entropy leads to an increase in T_g. If one of these factors is dominant, then a T_g change can occur in strained polymers. Beaucage et al. observed differences in the T_g for spun-cast polystyrene films with heating and cooling and attributed the T_g differences to residual strain in the cooled films.[61] However, for the epoxy films in this study, both heating and cooling cycles overlapped, suggesting that residual strain/stress effects were not present in these films. The epoxy resin was cured close to gelation before dissolving into PGMEA, but not past gelation, so the network backbone will still have mobility. Because of a very slow cure cycle and extensive annealing (9 h at T_g + 100 °C) before the thermal expansion measurements, we expect that spin-induced distortions in network structure were annealed away. We admit that the cure cycle can influence the microstructure of the network films, and potentially the thin film properties, but this must be investigated further.

Conclusions

Epoxy films of various thickness were spun onto silicon wafers with different surface treatments. Films thinner than 200−400 Å exhibited reduced thermal expansion relative to the thick films. This distance corresponds to a range of 10−20 end-to-end cross-link junctions. The reduction in the thermal expansion was *independent* of the substrate surface treatment which varied in both the surface energy and the interaction strength with the polymer, suggesting that network cross-links have a significant influence on the thin film thermal behavior and can screen or dampen the influence of the polymer/substrate interaction. The expansion data can be fit assuming a "glassy" layer exist near the wafer surface with significantly reduced thermal expansion. The thickness of this assumed "glassy" layer was ≈50 Å, a distance corresponding to 2−3 cross-links. The thickest epoxy films displayed rubbery thermal expansion values for temperatures above the bulk polymer glass transition temperature. However, with each surface treatment, the thinnest epoxy films (<120 Å) exhibited typical glassy expansion values even at temperatures 20−40 °C above the bulk polymer glass transition temperature.

References and Notes

(1) ten Brinke, G.; Ausserre, D.; Hadziioannou, G. *J. Chem. Phys.* **1988**, *89*, 4374.
(2) Kumar, S. K.; Vacatello, M.; Yoon, D. Y. *J. Chem. Phys.* **1988**, *89*, 5206.
(3) Wallace, W. E.; Beck, Tan N. C.; Wu, W. L.; Satija, S. *J. Chem. Phys.* **1998**, *108*, 3978.
(4) Yu, C.-J.; Richter, A. G.; Datta, A.; Durbin, M. K.; Dutta, P. *Physica B* **2000**, *283*, 27.
(5) van der Lee, A.; Hamon, L.; Holl, Y.; Grohens, Y. *Langmuir* **2001**, *17*, 7664.
(6) Mayes, A. M. *Macromolecules* **1994**, *27*, 3114.
(7) Brown, H. R.; Russell, T. P. *Macromolecules* **1996**, *29*, 798.
(8) Tanaka, K.; Taura, A.; Ge, S.-R.; Takahara, A.; Kajiyama, T. *Macromolecules* **1996**, *39*, 3040.
(9) Calvert, P. *Nature (London)* **1996**, *384*, 311.
(10) Reiter, G. *Europhys. Lett.* **1993**, *23*, 579.
(11) Reiter, G. *Macromolecules* **1994**, *27*, 3046.
(12) Orts, W. J.; van Zanten, J. H.; Wu, W.-L.; Satija, S. K. *Phys. Rev. Lett.* **1993**, *71*, 867.
(13) Fryer, D. S.; Nealey, P. F.; de Pablo, J. J. *Macromolecules* **2000**, *33*, 6439.
(14) Keddie, J. L.; Jones, R. A.; Cory, R. A. *Faraday Discuss.* **1994**, *98*, 219.
(15) Prucker, O.; Christian, S.; Bock, H.; Ruhe, J.; Frank, C. W.; Knoll, W. *Macromol. Chem. Phys.* **1998**, *199*, 1435.
(16) Kawana, S.; Jones, R. A. L. *Phys. Rev. E* **2001**, *63*, 021501-1.
(17) Tsui, O. K. C.; Zhang, H. F. *Macromolecules* **2001**, *34*, 9139.
(18) Tsui, O. K. C.; Russell, T. P.; Hawker, C. J. *Macromolecules* **2001**, *34*, 5535.
(19) Fakao, K.; Miyamoto, Y. *Phys. Rev. E* **2000**, *61*, 1743.
(20) Tate, R. S.; Fryer, D. S.; Pasqualini, S.; Montague, M. F.; de Pablo, J. J.; Nealey, P. F. *J. Chem. Phys.* **2001**, *115*, 9982.
(21) Wallace, W. E.; van Zanten, J. H.; Wu, W. L. *Phys. Rev. E* **1995**, *52*, R3329.
(22) Keddie, J. L.; Jones, R. A. L.; Cory, R. A. *Europhys. Lett.* **1994**, *27*, 59.
(23) Fryer, D. S.; Peters, R. D.; Kim, E. J.; Tomaszewski, J. E.; de Pablo, J. J.; Nealey, P. F.; White, C. C.; Wu, W. L. *Macromolecules* **2001**, *34*, 5627.
(24) van Zanten, J. H.; Wallace, W. E.; Wu, W. L. *Phys. Rev. E* **1996**, *53*, R2053.
(25) Soles, C.; Lin, E. K.; Lenhart, J. L.; Jones, R. L.; Wu, W.-L.; Goldfarb, D. L.; Angelopoulos, M. *J. Vac. Sci. Technol. B* **2001**, *19*, 2690.
(26) Forrest, J. A.; Dalnokin-Veress, K.; Stevens, J. R.; Dutcher, J. R. *Phys. Rev. Lett.* **1996**, *77*, 2002.
(27) Pochan, D. J.; Lin, E. K.; Satija, S. K.; Wu, W.-L. *Macromolecules* **2001**, *34*, 3041.
(28) Zheng, X.; Sauer, B. B.; van Alsten, J. G.; Schwarz, S. A.; Rafailovich, M. H.; Sokolov, J.; Rubinstein, M. *Phys. Rev. Lett.* **1995**, *74*, 407.
(29) Zheng, X.; Rafailovich, M. H.; Sokolov, J.; Strzhemechny, Y.; Schwarz, S. A.; Sauer, B. B.; Rubinstein, M. *Phys. Rev. Lett.* **1997**, *79*, 241.
(30) Lin, E. K.; Kolb, R.; Satija, Wu W.-L. *Macromolecules* **1999**, *32*, 3753.
(31) Frank, B.; Gast, A. P.; Russell, T. P.; Brown, H. R.; Hawker, C. *Macromolecules* **1996**, *29*, 6531.
(32) Palmese, G. R.; McCullough, R. L. *Composites A* **1999**, *30*, 3.
(33) Palmese, G. R.; McCullough, R. L. *J. Adhes.* **1994**, *44*, 29.
(34) Palmese, G. R.; McCullough, R. L. *J. Appl. Polym. Sci.* **1992**, *46*, 1863.
(35) Yim, H.; Kent, M.; McNamara, W. F.; Ivkov, R.; Satija, S.; Majewski, J. *Macromolecules* **1999**, *32*, 7932.
(36) VanLandingham, M. R.; Dagastine, R. R.; Eduljee, R. F.; McCullough, R. L.; Gillespie, J. W. *Composites A* **1999**, *30*, 75.
(37) Certain commercial equipment, instruments, or materials are identified in this paper in order to specify the experimental procedure adequately. Such identification is not intended to imply recommendation or endorsement by the National Institute of Standards and Technology, nor is it intended to imply that the materials or equipment identified are necessarily the best available for the purpose.

(38) Fukau, K.; Uno, S.; Miyamoto, Y.; Hoshino, A.; Miyaji, H. *Phys. Rev. E* **2001**, *64*, 051807.
(39) Wu, W.-L.; Bauer, B. J. *Macromolecules* **1986**, *19*, 1613.
(40) Wu, W.-L.; Hunston, D. L.; Yang, H.; Stein, R. S. *Macromolecules* **1988**, *21*, 756.
(41) Mansfield, K. F.; Theodorou, D. N. *Macromolecules* **1991**, *24*, 6283.
(42) Xie, L.; DeMaggio, G. B.; Frieze, W. E.; DeVries, J.; Gidley, D. W.; Hristov, H. A.; Yee, A. F. *Phys. Rev. Lett.* **1995**, *74*, 4947.
(43) Ge, S.; Pu, Y.; Zhang, W.; Rafailovich, M.; Sokolov, J.; Buenviaje, C.; Buckmaster, R.; Overney, R. M. *Phys. Rev. Lett.* **2000**, *85*, 2340.
(44) Liu, Y.; Russell, T. P.; Samant, M. G.; Stohr, J.; Brown, H. R.; Cossy-Favre, A.; Diaz, J. *Macromolecules* **1997**, *30*, 7768.
(45) Wallace, W. E.; Fischer, D. A.; Efimenko, K.; Wu, W.-L.; Genzer, J. *Macromolecules* **2001**, *34*, 5081.
(46) Starr, F. W.; Schroder, T. B.; Glotzer, S. C. *Phys. Rev. E* **2001**, *64*, 021802.
(47) Beck, Tan N. C.; McKnight, S. H.; Palmese, G. R. *Proc. Am. Chem. Soc.: Polym. Mater. Sci. Eng.* **1997**, *77*, 640.
(48) Frank, C. W.; Rao, V.; Despotopoulou, M. M.; Pease, R. F. W.; Hinsberg, W. D.; Miller, R. D.; Rabolt, J. F. *Science* **1996**, *273*, 912.
(49) Pearce, E. M.; Kwei, T. K.; Min, B. Y. *J. Macromol. Sci., Chem.* **1984**, *A21*, 1181.
(50) Prinos, J.; Panayiotou, C. *Polymer* **1995**, *36*, 1223.
(51) Yu, C.-J.; Richter, A. G.; Datta, A.; Durbin, M. K.; Dutta, P. *Phys. Rev. Lett.* **1999**, *82*, 2326.
(52) Evmenenko, G.; Dugan, S. W.; Kmetko, J.; Dutta, P. *Langmuir* **2001**, *17*, 4021.
(53) Mathew, Mate, C.; Novotny, V. J. *J. Chem. Phys.* **1991**, *94*, 8420.
(54) Briggman, K. A.; Stephenson, J. C.; Wallace, W. E.; Richter, L. J. *J. Phys. Chem. B* **2001**, *105*, 2785.
(55) Gautam, K. S.; Schwab, A. D.; Dhinojwala, A.; Zhang, D.; Dougal, S. M.; Yegeneh, M. S. *Phys. Rev. Lett.* **2000**, *85*, 3854.
(56) Hu, X.; Shin, K.; Rafailovich, M.; Sokolov, J.; Stein, R.; Chan, Y.; Williams, K.; Wu, W.-L.; Kolb, R. *High Perform. Polym.* **2000**, *12*, 621.
(57) Pae, K. D.; Tang, C. L.; Vijayan, K. *J. Mater. Sci.* **1986**, *21*, 2901.
(58) Saiz, E.; Riande, E.; Mark, J. E. *Macromolecules* **1984**, *17*, 899.
(59) Diaz-Calleja, R.; Riande, E.; Guzman, J. *J. Polym. Sci., Polym. Phys. Ed.* **1986**, *24*, 337.
(60) Diaz-Calleja, R.; Riande, E.; Guzman, J. *Polymer* **1987**, *28*, 2190.
(61) Beaucage, G.; Composto, R.; Stein, R. S. *J. Polym. Sci., Part B* **1993**, *31*, 319.

MA011903V